



Article

Study on Spray Deposition and Drift Characteristics of UAV Agricultural Sprayer for Application of Insecticide in Redgram Crop (*Cajanus cajan L. Millsp.*)

Yallappa Dengeru ¹, Kavitha Ramasamy ^{1,*}, Surendrakumar Allimuthu ¹, Suthakar Balakrishnan ¹, Ayyasamy Paramasivam Mohan Kumar ¹, Balaji Kannan ² and Kalarani Muthusami Karuppasami ³

¹ Department of Farm Machinery and Power Engineering, Agricultural Engineering College and Research Institute, Tamil Nadu Agricultural University, Coimbatore 641003, India

² Department of Physical Science and Information Technology, Agricultural Engineering College and Research Institute, Tamil Nadu Agricultural University, Coimbatore 641003, India

³ Directorate of Crop Management, Tamil Nadu Agricultural University, Coimbatore 641003, India

* Correspondence: kavitha@tnau.ac.in

Abstract: Insecticide applications are typically being carried out with traditional manual spraying equipment in redgram, which leads to inadequate control of insects due to higher crop height. The modern deployment of tractor-drawn spray machines causes serious damage to the crop. In this connection, unmanned aerial vehicle (UAV) spray technology has great potential for precise insecticide application in redgram crops. One of the important machine parameters influencing droplet deposition and drift characteristics in UAV sprayers is downwash airflow generated by a multi-rotor propeller. A field experiment was carried out at the redgram research field (N11.01, E76.92), Tamil Nadu Agricultural University, Coimbatore, Tamil Nadu, during 2021–2022 to study the spray drift and deposition characteristics of an autonomous UAV sprayer. The Imidacloprid (a.i. 17.8SL) insecticide mixed with water in a ratio of 1 mL per liter was sprayed with a UAV sprayer. Water-sensitive paper samples were kept at upper, middle, and bottom positions on the leaves, and data were analyzed for the spray droplet size, deposition rate, droplet density, and area coverage both in target and non-target areas using Spray Deposit Scanner software. UAV spray droplet deposition rate (2.93 ± 0.17 , 2.01 ± 0.08 , and 2.21 ± 0.16 $\mu\text{L cm}^{-2}$), droplet density (47 ± 4.04 , 53 ± 3.61 , and 52 ± 8.74 droplets cm^{-2}), and area coverage (15.72 ± 0.39 , 16.60 ± 0.71 , and $14.99 \pm 0.39\%$) were highest in the upper layer as compared to the middle layer (droplet deposition rate: 1.21 ± 0.08 , 1.07 ± 0.03 , and $0.77 \pm 0.02 \mu\text{L cm}^{-2}$; droplet density: 42 ± 2.52 , 43 ± 8.50 , and 38 ± 2.52 droplets cm^{-2} ; area coverage: 10.95 ± 0.81 , 11.22 ± 0.56 , and $8.57 \pm 0.44\%$) and bottom layer (droplet deposition rate: 0.41 ± 0.06 , 0.35 ± 0.03 , and $0.33 \pm 0.03 \mu\text{L cm}^{-2}$; droplet density: 22 ± 4.36 , 17 ± 3.51 , and 19 ± 4.51 droplets cm^{-2} ; area coverage: 2.78 ± 0.29 , 2.95 ± 0.45 , and $2.46 \pm 0.20\%$, respectively). In the spray drift test, there was a higher droplet deposition rate (1.63 ± 0.09 , 1.93 ± 0.05 , and $1.82 \pm 0.06 \mu\text{L cm}^{-2}$), area coverage (14.40 ± 0.07 , 17.54 ± 0.36 , and $16.42 \pm 0.30\%$), and droplet density (46 ± 3.61 , 54 ± 2.08 , and $45 \pm 3.21 \text{ No's cm}^{-2}$) in the target area as compared to the non-target area (droplet deposition rate: 0.88 ± 0.02 , 0.46 ± 0.03 , 0.22 ± 0.05 , and $0.00 \mu\text{L cm}^{-2}$; droplet density: 23 ± 1.53 , 11 ± 2.08 , 6 ± 1.53 , and 0.00 droplets cm^{-2} ; area coverage: 7.58 ± 0.34 , 4.41 ± 0.19 , 2.16 ± 0.05 , and 0.00% , respectively), which may have been due to the downwash airflow produced by the multi-rotor propeller of the UAV sprayer. Finally, the UAV-based spraying technology results showed that the downwash air produced by the six-rotor propeller improved the penetrability of insecticide to crop leaves and led to a higher droplet deposition rate, droplet density, area coverage, and droplet penetrability on the upper layer, middle layer, and bottom layer of the plants.

Keywords: droplet size; deposition rate; downwash airflow; flat fan nozzle; redgram leaf; UAV sprayer



Citation: Dengeru, Y.; Ramasamy, K.; Allimuthu, S.; Balakrishnan, S.; Kumar, A.P.M.; Kannan, B.; Karuppasami, K.M. Study on Spray Deposition and Drift Characteristics of UAV Agricultural Sprayer for Application of Insecticide in Redgram Crop (*Cajanus cajan L. Millsp.*). *Agronomy* **2022**, *12*, 3196. <https://doi.org/10.3390/agronomy12123196>

Academic Editors: Xiongkui He, Fuzeng Yang and Baijing Qiu

Received: 19 September 2022

Accepted: 19 October 2022

Published: 16 December 2022

Publisher's Note: MDPI stays neutral with regard to jurisdictional claims in published maps and institutional affiliations.



Copyright: © 2022 by the authors. Licensee MDPI, Basel, Switzerland. This article is an open access article distributed under the terms and conditions of the Creative Commons Attribution (CC BY) license (<https://creativecommons.org/licenses/by/4.0/>).

1. Introduction

The pigeon pea or redgram (*Cajanus cajan L. Millsp.*) is the second most significant pulse crop and a rich source of protein. It is mainly intercropped with pulses, cereals, millets, and oilseeds. Conventional methods of insecticide and pesticide spray application lead to excessive application of chemicals, lower spray uniformity, deposition, and coverage, resulting in a higher cost of pesticide as well as environmental pollution, as well as increased drudgery and reduced area coverage [1]. Application of insecticide is being carried out with traditional spraying equipment on the redgram crop, which leads to inadequate control of pests due to higher crop height. On the other hand, tractor-drawn spray machines cause serious damage to the crop. Unmanned aerial vehicle (UAV) spray technology has a great potential for precise insecticide application in red gram crops.

UAV spray technology is one that can be controlled by a pilot on a ground station autonomously using pre-programmed flight plans [2–4]. The UAV is attached with spray tanks, which can store the insecticide and pesticide and spray them over the crops. These fly at the proper height, helping the pesticide penetrate perfectly into the crop [5–7]. The most essential benefit of using a multi-rotor UAV for chemical spraying is that, due to its unique rotor structure and principle of motion, it generates a powerful downwash airflow during flight operation, changing the crop disturbance and improving liquid penetration [8,9]. It has been reported that liquid sprayed using UAVs has quite a good deposition impact on the bottom part of crops [10–13].

Many investigators have carried out research on the spray effects of UAV spray technology. For insecticides sprayed by UAV sprayers, droplet size is one of the most important factors affecting droplet drift and deposition rate [14,15]. Wind speed is one of the meteorological conditions that might cause spray drift [16,17]. The UAV machine operation parameters, viz., flight height, travel speed, payload, and configuration of the UAV model, have a great impact on the distribution and penetration of droplets [18]. The height and forward speed of UAV flight parameters have a great impact on the spray droplet distributions [19,20]. The downwash airflow velocity produced by the rotors can create a strong velocity distribution for plants during spraying, helping spray droplets to atomize much further with enhanced deposition onto the crop surface. As a result, spray droplet velocity has positive effects on spray swath, deposition, and drift [21–23]. Shengde et al. [24] used a wind velocity sensor to evaluate the effect of rotor wind field on the uniformity and penetration of droplet deposition in three spatial directions: X, Y, and Z. Spray droplet drift is decreased, and the impact of droplet deposition rate is increased when chemicals are applied with a UAV sprayer [25,26]. Spray drift from unmanned aerial vehicles (UAVs) was studied at various pressures (2, 3, 4, and 5 bar). Liu et al. [27] studied spray drift from unmanned aerial vehicles (UAVs) at various pressures (2, 3, 4, and 5 bar). The drift typically dropped, increasing the distance downwind from the UAV test platform. Berner and Chojnacki [28] conducted the tests on the relationship between the speed of the UAV rotor and spray deposition. Fritz et al. [29] tested the effects of spray rate and droplet size on droplet deposition on wheat and found that lower spray rates with larger droplet sizes resulted in greater deposits. It has been reported that liquid sprayed using UAV has quite a good deposition impact on the bottom part of crops [10,30]. When the flying height increases, the vertical velocity of the UAV downwash flow near the crop canopy will decrease [31]. The rotor wind field, flight environment (temperature, humidity, wind direction, and wind power), equipment performance, and pesticide characteristics (viscosity, density) also have an effect on the spraying effect [32–34]. Xinyu et al. [35] evaluated UAV spray and deposition in a rice field using Z-3 UAV operating parameters that could control 90% of drift in 8 m. Yang et al. [36] studied the influence of UAV rotor downwash airflow spray width using the XV-2 model. The results showed that UAV flight height mainly influenced the spray width, and the effective spray width was 10.0 m at a flight height of 6.0 m and had better effect on droplet deposition at 2.0 m height of spray. When droplets below 200 m are subjected to a 5 km/h crosswind, they can drastically deviate from their intended path [37]. Choi et al. [38] conducted tests using a six-rotor UAV

with three heights and two speeds of operational parameters. Lan et al. [39] conducted research on the impact of the UAV downwash on droplet deposition distribution using a DJI T16 UAV, and it was found that with an increase in flight height, the change of the downwash wind field led to a gradual decrease in droplet deposition in the effective spray area and were deposited more uniformly [24,27]. For decades, empirical and mechanistic models have been developed to predict pesticide deposition and drift from aerial pesticide application [40–42]. In insect control operations, the quality of insecticide application is important. The proper dosage should be applied uniformly, the toxicant should reach the target, and droplet size and density on the target should be correct [43]. The aim of this investigation was to explore the spray droplet deposition rate, droplet size, droplet density, area coverage, uniformity distribution, and drift characteristics in the redgram crop sprayed by a UAV sprayer. It also provides technical reference and guidance for proper and safe aerial spraying in agricultural production.

2. Materials and Methods

2.1. Equipment

The UAV used in the present investigation was an E610P six-rotor electric (M/s. EFT Electronic Technology Co., Ltd., Hefei City, China), as shown in Figure 1. The spraying system of the UAV sprayer mainly consists of BLDC motors, lithium polymer (LiPo) batteries, a flight controller, an RC receiver, a GNSS RTK GPS unit, a pesticide tank, a pump, nozzles, and a supporting frame. The UAV sprayer has two LiPo batteries of 6 cells each, with a capacity of 16,000 mAh to supply the necessary current required for the propulsion system. A 24 V BLDC motor coupled with a pump was used to pressurize spray liquid and then to atomize it into fine spray droplets. This UAV sprayer has four numbers of 2020A-132 series flat fan nozzles (M/s. Ningbo Licheng Agricultural Spray Technology Co., Ltd., Zhejiang, China), which are mounted and screwed below the BLDC motor base plate. This UAV model has the functions of GPS route planning and breakpoint return, which can complete aerial spraying operations autonomously. The main performance indicators are shown in Table 1.



Figure 1. Six-rotor electric autonomous UAV sprayer.

2.2. Field Plot

The experiment was carried out at the redgram research field (N11.01, E76.92), Department of Pulses, Tamil Nadu Agricultural University, Coimbatore, Tamil Nadu state, India. The details of crop parameters are mentioned below in Table 2. The redgram crop parameters were average row to row, plant to plant spacing, and average crop height measured during the UAV spraying operation. Figure 2 depicts the application of insecticide in the redgram crop using a UAV agricultural sprayer.

Table 1. Specifications of UAV agricultural sprayer.

Main Parameter	Norms and Numerical Value
Type	Hexacopter
Item model	E610P
Unfold fuselage size, (L × W × H), mm	2000 × 1800 × 670
Folding size, (L × W × H), mm	950 × 850 × 670
Power source	12S 160,000 mAh LiPo Battery
Payload capacity, L	10
Self-weight, kg	6.9
Take-off weight, kg	26
Flight height, m	1–20
Forward travel speed, ms ⁻¹	0–8
Type of spray nozzle	Flat fan shape (2020A-132 series)
Number of nozzles	4
Discharge rate, l m ⁻¹	0–3.2
Swath width of spray, m	3–5
Liquid pressure, kg cm ⁻²	3.4
Remote controller distance, km	1.5
No-load flight time, min	25
Charging time, min	90

Table 2. Details of crop parameters.

Crop Parameters	
Crop	Redgram
Variety	Co8
Plot size (L × W), mm	70 × 40
Height of crop, m	1.9 to 2.3
Stage of crop	>110 DAS
Row to row spacing, m	0.70 to 0.74
Plant-to-plant spacing, m	0.15 to 0.21

**Figure 2.** UAV agricultural spray operation in redgram crop.

2.3. Spray sampling Scheme

2.3.1. Sampling of Spray Deposition

Water-sensitive papers (produced by AAMS, Maldegem, Belgium) are a kind of spray card specifically designed for visualizing deposit patterns. It has a dye-coated surface that produces visible stains from aqueous droplets, and we used a 50×50 mm WSP to collect the amount of spray droplets deposition on the surface of the leaves in three locations [44,45]. At each sampling point, the WSP was clamped with a double-ended clip and kept on the leaves at three different heights of the plants, viz., 40 cm, 110 cm, and 210 cm from the ground level. The arrangement and locations of WSP samples on redgram leaf are shown in Figure 3a,b. The field layout with the location of WSP spray deposition samples is shown in Figure 4.

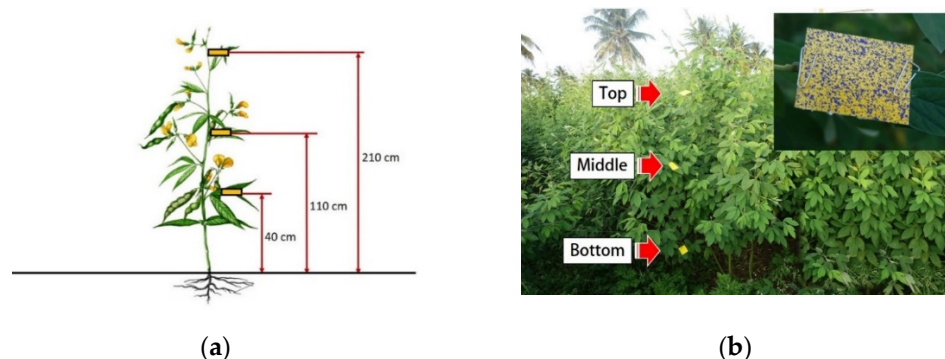


Figure 3. Layout and position of water sensitive paper for the collection of spray droplet deposition characteristics: (a) layout of WSP samples in the upper, middle, and bottom at 210, 110, and 40 mm height from the ground, respectively, and (b) the position of WSP samples on redgram leaf in the field.

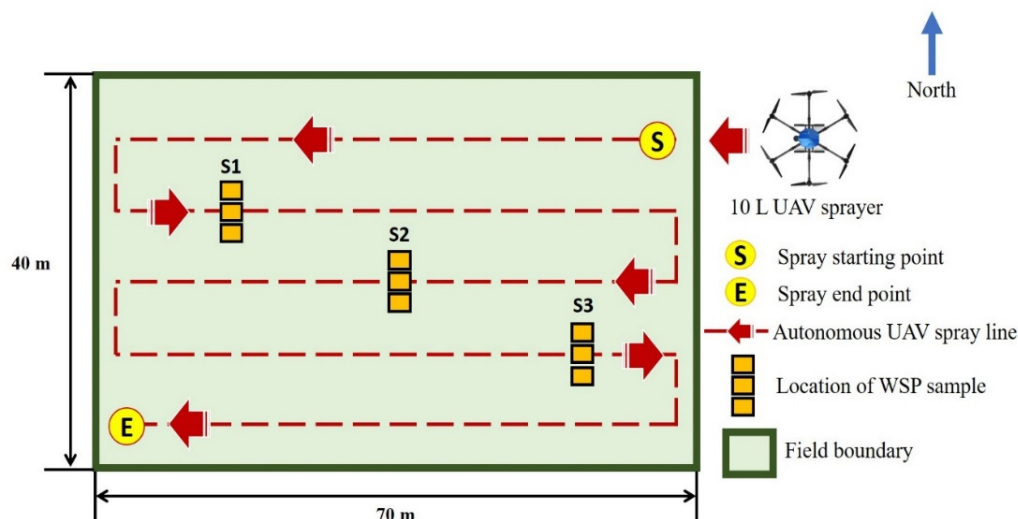


Figure 4. Schematic diagram for the location of WSP spray.

2.3.2. Sampling of Spray Drift

The UAV agricultural spray drift experiment was conducted from 09:50 a.m. to 10:30 a.m. on 8 December 2021 at the redgram research field (N11.01, E76.92), Tamil Nadu Agricultural University, Coimbatore, Tamil Nadu state, India. Weather conditions, viz., wind velocity, air temperature, and relative humidity, were recorded during the spray drift experiment in the redgram field [46]. A WSP with a size of 50×50 mm was placed on flat iron plate attachments to square iron rods at all collection points for the measurement of spray droplet deposition rate in the canopy. The height of WSP samples were adjusted to the head of the redgram crop canopy by flexible clamps [25], as shown in Figure 5a,b.

A transmitter (SKYDROID, T10 2.4 Hz 10CH FHSS) with a screen recorded the flight deviation, travel speed, and altitude of each flight using ground station equipment. The total length of the target sample line was close to three meters, which is greater than the effective spraying width calibrated during the laboratory test. The water-sensitive paper collection cards were mounted below the UAV autonomous spray line fixed at 0 m, and with consideration of the natural wind direction, single-line WSP collection cards were placed and spaced at -1.0, 0.0, and -2.0 m on the upside wind flow direction of the UAV path line, whereas another set of five WSPs collection cards were placed at 1.0, 2.0, 3.0, 4.0, and 5.0 m on the down side of the wind flow [12,25]. The schematic experimental layout of WSP drift sample locations is shown in Figure 6.

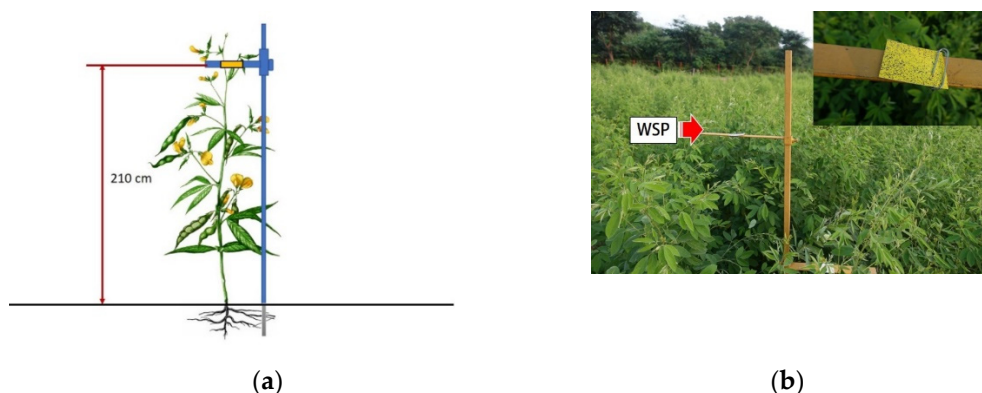


Figure 5. Placement of WSP sample for spray drift: (a) layout position of WSP sample on iron stand at 210 mm distance from the ground level, and (b) position of the WSP sample iron stand in the redgram field crop.

2.4. Selection and Feeding of UAV Spray Operational Parameters

The nozzle 2020A-132 series flat fan nozzles (M/s. Ningbo Licheng Agricultural Spray Technology Co., Ltd., Zhejiang, China) were selected for the test [47]. When the UAV is spraying, the four nozzles behind the fuselage are turned on for spraying. The spray flow rate of four nozzles were tested using a handheld portable-type sensor-based digital nozzle tester (AAMS, Maldegem, Belgium). For measuring liquid operating pressure, a digital liquid pressure gauge was connected to the output of a water spray hose pipe, and the other end was connected to the nozzles of the lateral hose pipe. The maximum flow rate of single nozzles was measured at 0.8 l m^{-1} at 100% spray motor speed, and the total nozzle flow rate and liquid pressure, including the four nozzles, were 3.2 l m^{-1} and 3.4 kg cm^{-2} , respectively. The height of spray of 1.6 m (vertical distance between the crop canopy and the tip of the drone sprayer nozzle) was set for the complete spray operation. The height of spray and crop height layout is shown in Figure 7. The main sucking insects were leafhoppers and white flies in the redgram crop. Imidacloprid insecticide was mixed with water in a ratio of 1 mL per liter (as per the redgram crop package of practice published by the Tamil Nadu Agricultural University, Coimbatore, India). The diluted chemical was sprayed, and operational parameters during the spraying time are presented in Table 3.

Table 3. UAV sprayer operational parameters.

Operational Parameters	Norms and Numerical Values
Forward speed, ms^{-1}	3
Height of spray, m	1.6
Swatch width of spray, m	3.8
Discharge rate, l m^{-1}	3.2
Liquid pressure, kg cm^{-2}	3.4

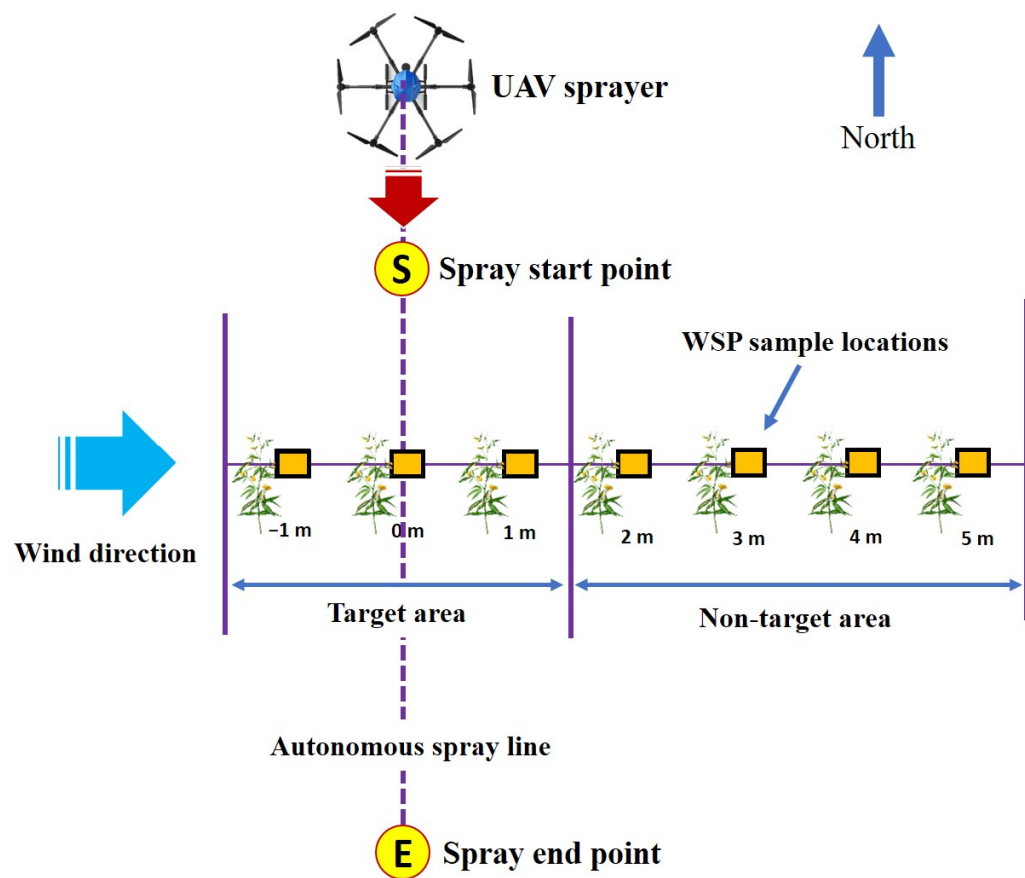


Figure 6. Schematic experimental layout of WSP drift sample locations.

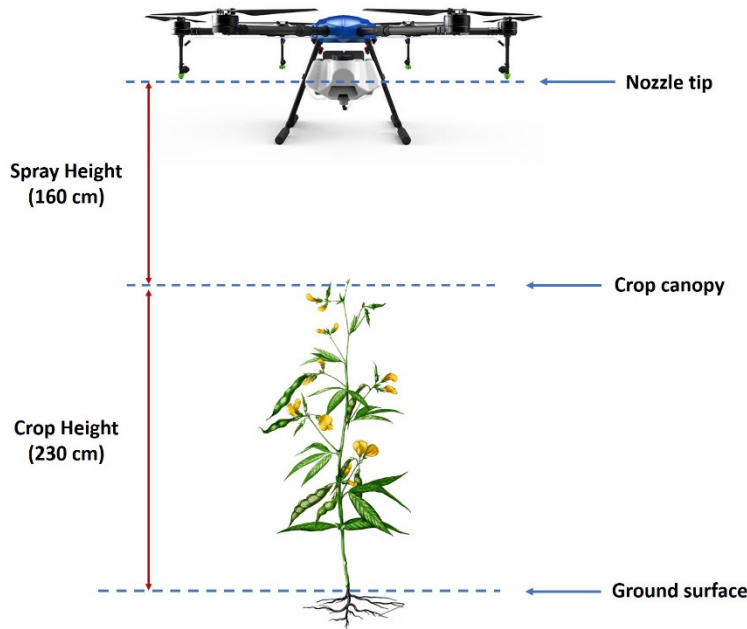


Figure 7. Schematic experimental layout of height of spray and crop height.

2.4.1. Autonomous Spraying System

The Agri Assistant mobile app (JIYI K++V2, V1.5.1) was used for UAV autonomous spraying operations in the redgram field. It also provides the live status of the UAV spray

operational parameters, viz., field GPS location and satellite connection strength, field area, time required to spray a given area, battery voltage warning, spray motor speed, height of flight, and spray swath width. Initially, the GPS co-ordinates of the redgram field boundary such as latitude, longitude, and altitude were entered. The operational parameters of the UAV sprayer, viz., flight forward speed, spray height, spray swath width, and nozzle flow rate were chosen as input operation modes for the spray test. Normal operation conditions, such as a flight speed of 3 ms^{-1} and a flight height of 1.6 m above the crop canopy with a swath width of 3.8 m, were used to ensure the validity and authenticity of the test results [25]. After providing the field boundary and spray operational parameters to the Agri Assistant app, the UAV sprayer starts in auto take-off mode and begins its spraying operation by clicking the auto take-off option on the Agri Assistant mobile device at the ground station. The UAV autonomous spraying operation of the Agri Assistant app screen is shown in Figure 8. The layout of predefined and actual autonomous spray path map layout is shown in Figure 9.

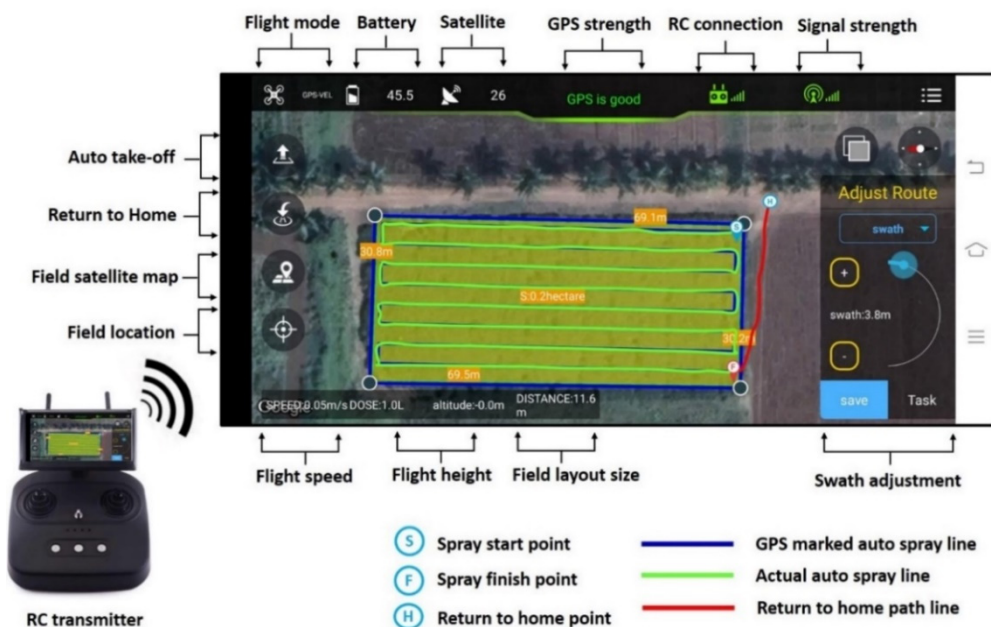


Figure 8. Screen view of the Agri Assistant mobile app for UAV autonomous spraying operations.

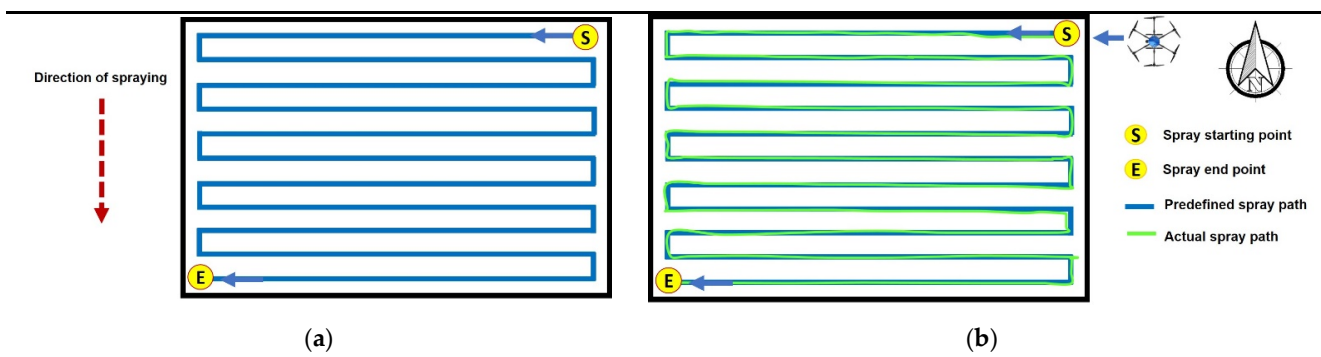


Figure 9. Field maps of UAV spray operation with autonomous mode. (a) Predefined autonomous spray path map. (b) Actual autonomous spray path map.

2.4.2. Recording of Meteorological Parameters

During UAV spraying operations, the different meteorological parameters such as wind velocity, air temperature, humidity, and rainfall meteorological parameters were

recorded in order to avoid the ill effects of climate on the performance of the spraying operation [16]. A portable anemometer (LUTRON AM 4202, Vane type, rang: 0.4~30.0 ms⁻¹) was mounted on a square iron pipe at 2.0 m above the crop canopy to measure the wind velocity every 60 s [36]. Weather conditions, including wind speed, air temperature, and relative humidity, were recorded and are presented in Table 4.

Table 4. Meteorological data during the UAV spray test in the redgram field.

Date	8 December 2021	
Time	08:30 a.m. to 09:45 a.m.	
Location	Redgram research field (N11.01, E76.92), TNAU, Coimbatore, Tamil Nadu state, India	
Environmental parameters	Air temperature, °C	22.4 to 26.6°
	Relative humidity, %	56.2 to 61.1
	Wind velocity, ms ⁻¹	0.92 to 1.24
	Rainfall, mm	1.93 to 2.47 (drift experiment)

2.5. Collection of WSP and Spraying Effectiveness Analysis

After every spraying test, WSPs were collected and placed in marked envelopes one by one according to the serial number, then transferred to the laboratory for further study. The deposited amount and coverage density of the droplets at upper, middle, and bottom locations were analyzed as suggested by Zhu et al. [48].

2.5.1. Deposit Scan Software

WSPs were analyzed by using a Micro Droplet Analyzer and Macro Droplet Analyzer instruments (developed by LABLINE—DMS 101, India), and then images were processed with Deposit Scan software (developed by USDA, Wooster, OH, USA) [49]. The deposition rate ($\mu\text{L cm}^{-2}$); Dv0.1, Dv0.5, and Dv0.9 (μm); deposition density (No's cm^{-2}); and droplet penetrability (%) were studied. Mean deposition, mean deposition density, and coefficient of variation (CV) were also calculated. Dv0.1 is the droplet diameter (μm), wherein 10% of the spray volume contained in droplets was smaller than this value. Similarly, Dv0.5 and Dv0.9 are droplet diameters, wherein 50% and 90% of the spray volumes contained in the droplets were smaller than these values, respectively. The Dv0.5, also known as the volume median diameter (VMD), is the droplet size median at which the accumulation of all droplets, from small to large, equals 50% of the total volume of the droplets, which is a critical index to measure the size of the droplet [47]. Figure 10 depicts the step-by-step procedure for droplet size analysis using stereo micro and macro scope with Deposit scan software. The image processing procedure used in the study was similar to what Martin [50] reported previously. DepositScan software for finding droplet deposition rate ($\mu\text{L cm}^{-2}$) as per the work of Zhu et al. [48] is shown in Figure 11.

2.5.2. Droplet Penetrability (%)

In order to characterize the droplet penetrability between the various collection points in the experiment, this study measured the coefficient of variation (CV) of droplet deposition density at each collection point. The droplet penetrability was measured by the CV of the amount of droplet deposition on the upper, middle, and bottom layers of each collection point [44]. The smaller the CV value, the more uniform the droplet deposition and the better the penetration [51]. It was calculated by the following equation:

$$\text{Coefficient of Variation (CV)} = \frac{SD}{X} \times 100 \quad (1)$$

$$\text{Mean}(X) = \frac{\sum X_i}{N} \quad (2)$$

$$\text{Standard deviation (SD)} = \sqrt{\frac{\sum_1^N (X_i - X)^2}{N - 1}} \quad (3)$$

where

X is the deposition value of every sampling point ($\mu\text{L cm}^{-2}$);

X_i is the average deposition value of every sampling point ($\mu\text{L cm}^{-2}$);

N is the number of sampling points.

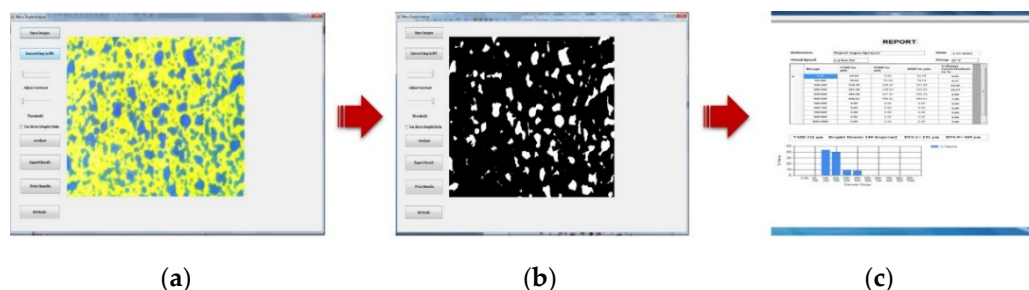


Figure 10. Procedure flow chart for droplet size analysis using stereo micro and macro scope: (a) image view of spray droplet sample under microscope; (b) conversion of the image to black and white and with adjustment of contrast and threshold; and (c) output results of volume mean diameter (VMD), droplet density (DD), and percentage of volume coverage.

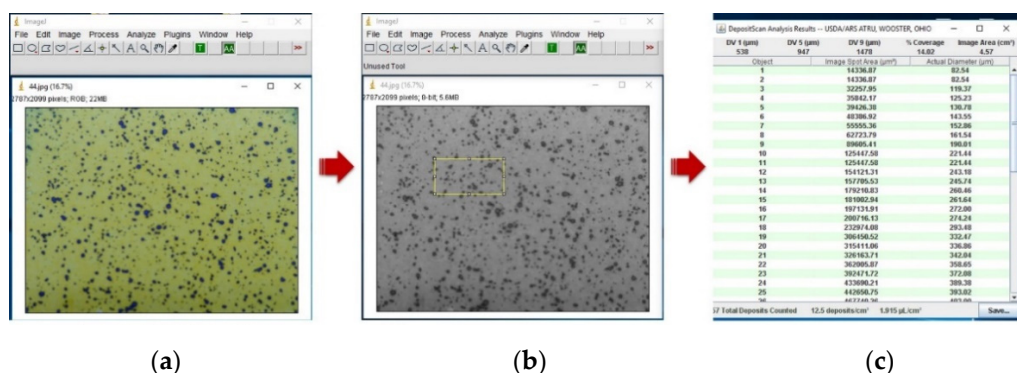


Figure 11. Flow chart for the procedure for droplet deposition rate under DepositScan software: (a) import of water-sensitive paper (WSP) image to Deposit Scan software, (b) conversion of the imported color images to black and white under 8 bit with the sample area marked, and (c) selection of the green AA Tool for analysis.

2.5.3. Effective Spray Width

The effective swath width is the distance between the points on either side of a single swath, wherein the rate of spray deposit equals one-half of the effective application rate. Effective spray width was determined in a manner that provided the most uniform overall application rate. The effective spray width test was performed according to the method described in the ASAE Standard [47].

2.5.4. Application Rate

The application rate was calculated as per the ASABE standard [52]. The mean value of discharge rate, travel speed, and effective spray width were measured, and application rate was calculated with the formula below:

$$\text{Application rate (R)} = \frac{Q \times K}{S \times W} \quad (4)$$

where

$$\begin{aligned}
 R &= \text{Application rate, } l \text{ ha}^{-1}; \\
 Q &= \text{Output rate, } l \text{ min}^{-1}; \\
 K &= \text{Constant, 600;} \\
 S &= \text{Travel speed, km h}^{-1}; \\
 W &= \text{Effective spray width, m}^3.
 \end{aligned}$$

3. Results and Discussion

3.1. Distribution and Analysis of Spray Droplet Deposition Characteristics

WSPs were placed on the leaf at 210 cm, 110 cm, and 40 cm above the ground level. The sampling locations were divided into upper, middle, and bottom layers. The average droplet deposition of each sample obtained by WSP analysis using DepositScan software is presented in Table 5.

Table 5. Characteristics of droplet deposition for each layer at each location.

WSP Position	Location of WSP	Spray Droplet Size (μm)			Droplet Density (No's cm^{-2})
		Dv0.1	Dv0.5	Dv0.9	
Upper	U1	200 \pm 9.45	423 \pm 5.03	508 \pm 5.69	47 \pm 4.04
	U2	223 \pm 5.29	472 \pm 2.65	622 \pm 3.00	53 \pm 3.61
	U3	236 \pm 4.36	492 \pm 5.57	724 \pm 6.51	52 \pm 8.74
Middle	M1	239 \pm 2.65	424 \pm 2.08	537 \pm 6.11	42 \pm 2.52
	M2	241 \pm 6.24	484 \pm 3.00	686 \pm 4.16	43 \pm 8.50
	M3	134 \pm 3.06	304 \pm 3.06	656 \pm 4.58	38 \pm 2.52
Bottom	B1	219 \pm 4.00	372 \pm 4.51	754 \pm 3.51	22 \pm 4.36
	B2	213 \pm 3.61	355 \pm 4.00	635 \pm 4.04	17 \pm 3.51
	B3	282 \pm 9.54	394 \pm 4.58	742 \pm 3.61	19 \pm 4.51

It is observed from Figure 12 that the droplet deposition rate decreased from the upper to the bottom layer, and droplet deposition rate in the upper (2.93 ± 0.17 , 2.11 ± 0.08 , and $2.36 \pm 0.16 \mu\text{L cm}^{-2}$), middle (1.22 ± 0.08 , 1.07 ± 0.03 , and $0.76 \pm 0.02 \mu\text{L cm}^{-2}$), and bottom layers (0.43 ± 0.06 , 0.35 ± 0.03 , and $0.32 \pm 0.03 \mu\text{L cm}^{-2}$) were found in locations 1, 2, and 3, respectively. The coverage per unit area decreased from the upper layer to the bottom layer. Coverage per unit area in the upper (15.72 ± 0.49 , 16.60 ± 0.71 , and $14.94 \pm 0.39\%$), middle (10.95 ± 0.81 , 11.22 ± 0.56 , and $8.57 \pm 0.44\%$), and bottom layers (2.78 ± 0.29 , 2.95 ± 0.45 , and $2.46 \pm 0.20\%$) was found in locations 1, 2, and 3, respectively. As shown in Table 5, the droplet deposition density on the upper (47 ± 4.04 , 53 ± 3.61 , and 52 ± 8.74 droplets cm^{-2}), middle (42 ± 2.52 , 43 ± 8.50 , 38 ± 2.52 droplets cm^{-2}), and lower layers (22 ± 4.36 , 17 ± 3.51 , and 19 ± 4.51 droplets cm^{-2}) was found in locations 1, 2, and 3, respectively. Overall, the droplet deposition density was the highest in the upper layer and the lowest in the middle and bottom layers. Yang et al. [53] found that the RPAAS rotor's downwash airflow generated a pressure difference between the top and lower surfaces of the leaf, resulting in torque and allowing spray droplets to penetrate up to fourfold to the bottom surface of the leaf. The droplet penetrability is another typical index to evaluate the deposition effect. In smaller CV, more uniform distribution of the spray droplet was observed. The best droplet penetrability was assessed on the basis of the coefficient of variation. The droplet penetrability was best in the upper layer, with the CV of deposition density reaching 6.34% compared to the middle and bottom layers at 6.45% and 13.02%, respectively. The findings of this research are in line with previous research and hence confirms that downwash and wind turbulence caused by RPAAS aircraft rotor blades aid in droplet deposition and canopy penetration [11,22,54–57].

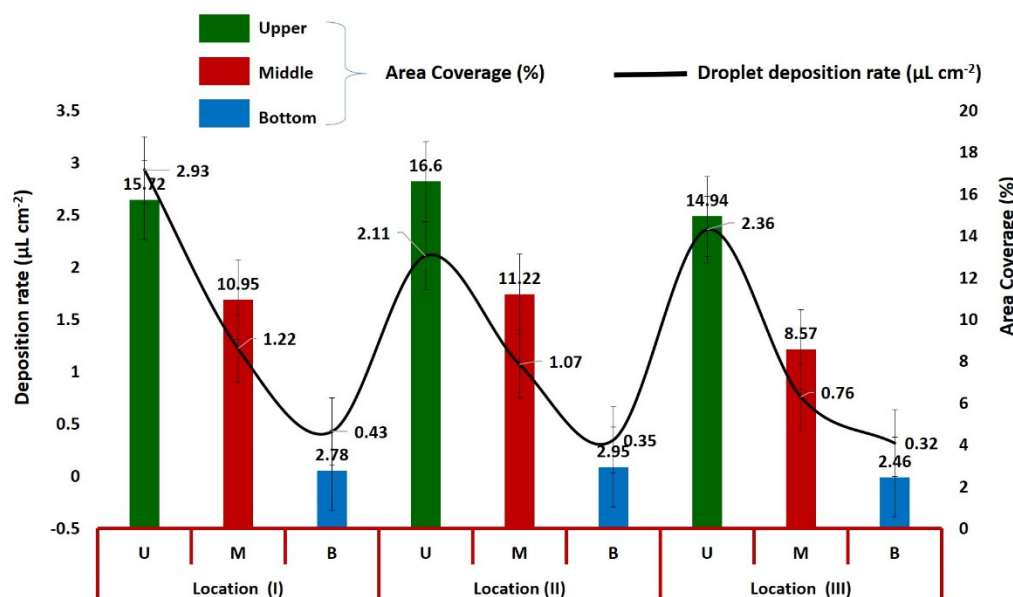


Figure 12. Droplet deposition rate and area coverage.

3.2. Effective Spray width and Application Rate of Chemical Usage

The average effective spray width was found to be 3100 mm at a height of spray of 1200 mm from the above crop canopy. It was observed that the swath width increased by increasing the height of spray and operating pressure. In addition, when the flight height was 1.0 to 3.0 m, the effective spray width was 3.1 to 3.8 m. This is in line with the earlier study [51].

The average 3 ms^{-1} travel speed was maintained during autonomous spray operation, and the actual field capacity of the UAV sprayer was found to be 2.84 ha h^{-1} .

The theoretical application rate was calculated as per the procedure explained in 2.5.4, and it was found to be 57.34 l ha^{-1} . The actual application rate was found to be 54.0 l ha^{-1} ($\approx 15.0 \text{ L}$ diluted chemical was consumed for covering 0.28 ha area of redgram field). This diluted imidacloprid (a.i. 17.8SL) chemical application rate was matched as per the recommendation of the redgram crop package of practice published by Tamil Nadu Agricultural University, Coimbatore, India. UAV spray droplet deposition drift results in target and non-target area zones.

For UAV spray drift, the sampling area was divided into two zones on the basis of the direction of the natural wind. The samples in the target area zone were placed at $-1.0, 0.0$, and 1.0 m distances, and the samples in the non-target area zone were placed at $2.0, 3.0, 4.0$, and 5.0 m distances, as presented in Table 6.

Table 6. Amount of spray drift droplet deposition.

Sample Zone	Drift Sample Distance (m)	Droplet Density (No's cm^{-2})
Target area	-1.0	46 ± 3.61
	0.0	54 ± 2.08
	1.0	45 ± 3.21
	2.0	23 ± 1.53
Non-target area	3.0	11 ± 2.08
	4.0	6 ± 1.53
	5.0	0.00

Figure 13 shows that the large amount of droplets were deposited at sampling points of -1.0 , 0.0 , and 1.0 m distance. Samples in the target area were found at 1.63 ± 0.09 , 1.93 ± 0.05 , and $1.82 \pm 0.06 \mu\text{L cm}^{-2}$, respectively, indicating that the droplets mainly deposited below the UAV sprayer flight route. This may have been due to the downwash air produced by the propeller of the UAV sprayer [55–57]. Li et al. [21] reported that the downwash air velocity had effects on droplet deposition and standing crop. A few droplets were also collected on WSPs in the non-target area zone because the droplets drifted with the wind to the downwind side. The droplet deposition in the non-target area samples, viz., 2.0 , 3.0 , 4.0 , and 5.0 m, were found to be 0.88 ± 0.02 , 0.46 ± 0.03 , 0.22 ± 0.05 , and $0.00 \mu\text{L cm}^{-2}$, respectively. From Figure 13, it is observed that the amount of droplet deposition decreased as lateral distance increased from the central line of flight path and was almost nil at 5.0 m from the UAV flight center line. The results support the findings of Bird et al. [58], who concluded that, under identical stability situations, increased wind speeds are likely to increase off-target deposition. Spraying droplets of UAV is affected by many factors, and the droplet size is one of them [17,59]. The ideal droplet size is 50 – $300 \mu\text{m}$. If the droplet size was less than $50 \mu\text{m}$, the droplets would be easy to drift. The effect of height, velocity, and nozzle flow rate on droplet dispersion during drone operation is proportional to crop canopy height [60]. If the droplet size is greater than $300 \mu\text{m}$, the droplets would find it difficult to penetrate the crop canopy and adhere to the target. As indicated by Bergeron et al. [37], our findings show that droplet size distribution may have a major impact on spray drift.

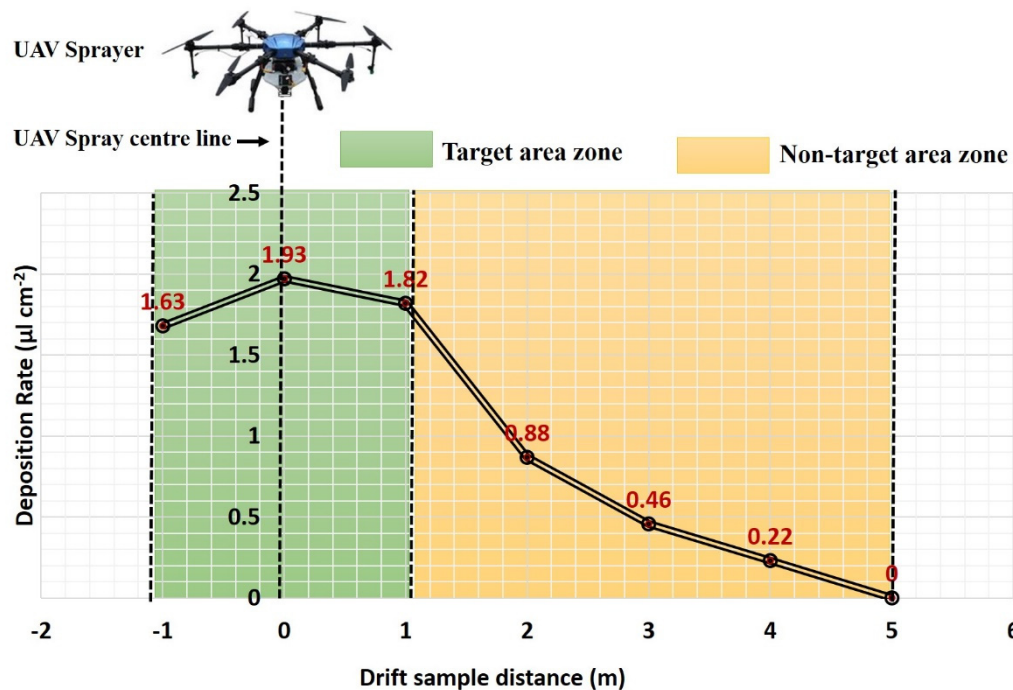


Figure 13. Droplet deposition at different drift sampling distances.

Table 6 and Figure 14 show that the large amount of droplet density and coverage area were found at sampling points of -1.0 , 0.0 , and 1.0 m distance. Samples of droplet density in the target area (-1.0 m to 1.0 m) were found at 46 ± 3.61 , 54 ± 2.08 , and $45 \pm 3.21 \text{ No's cm}^{-2}$, and 23 ± 1.53 , 11 ± 2.08 , 6 ± 1.53 , and $0.00 \text{ No's cm}^{-2}$ droplet density were found in the non-target area (2.0 m to 5.0 m). Similarly, more area coverage (%) was found in the target area at 14.40 ± 0.07 , 17.54 ± 0.36 , and $16.42 \pm 0.30\%$ compared to the non-target area at 7.58 ± 0.34 , 4.41 ± 0.19 , 2.16 ± 0.05 , and 0.00% , indicating that the droplets were mainly found more so below the UAV sprayer flight route (target area). This may have been due to the downwash air produced by the propeller of the UAV sprayer [11,54,60]. Yang [10] reported that the downwash air velocity had effects on area

coverage and droplet density on crop leaf. Few droplets were also collected on WSPs in the non-target area zone because the droplets drifted with the wind to the downwind side. According to other studies [55–57,61], the reason for the difference in droplet deposition results could have been that droplets with smaller sizes are more likely to drift outside the target area due to the influence of the environmental wind, whereas droplets with larger sizes, which are less affected by the environmental wind due to the mass of the droplet, are more likely to be deposited in the target area.

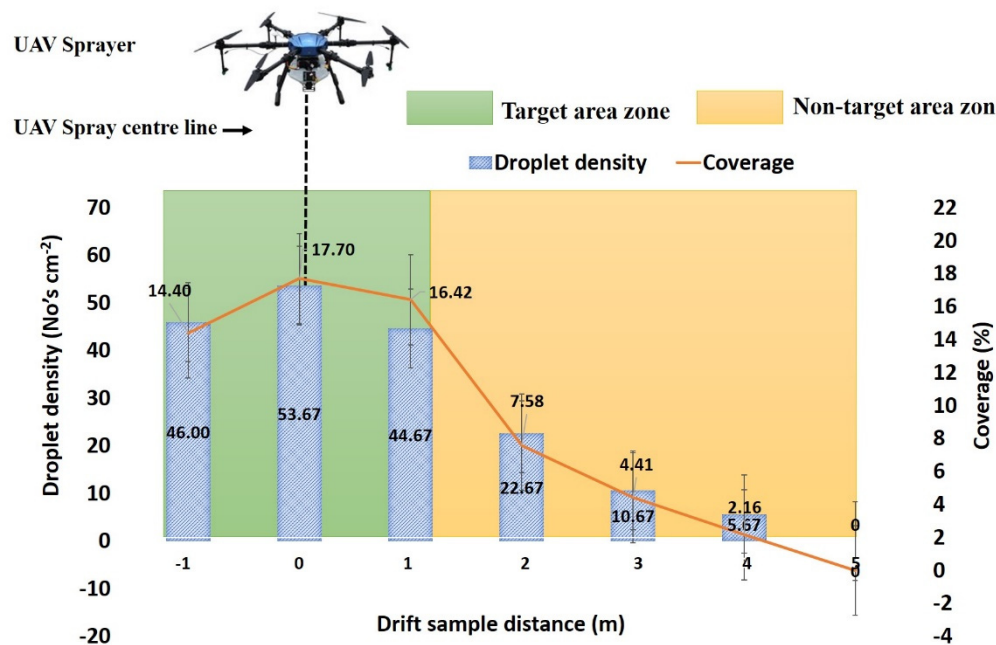


Figure 14. Droplet density and coverage at different drift sampling distances.

From Figure 14 and Table 4, it is observed that the amount of droplet density and area coverage were decreased as lateral distance increased from the central line of the flight path. Area coverage and droplet density were almost nil at 5.0 m from the UAV flight center line. These findings were comparable to those of Fritz [17], indicating that higher wind speed resulted in greater downwind ground deposition. The findings revealed that wind speed was the most important meteorological element in the transport and destiny of aerially applied sprays.

4. Conclusions

In this study, a multi-rotor UAV sprayer with a payload capacity of 10 liters was used in fully autonomous mode to apply insecticide to a redgram crop. The average deposition rate and area coverage in the upper layer were higher ($2.47 \mu\text{L cm}^{-2}$) when compared to the middle layer ($1.02 \mu\text{L cm}^{-2}$) and bottom layers ($0.37 \mu\text{L cm}^{-2}$) of redgram leaf. Overall, the droplet deposition rate ($2.47 \mu\text{L cm}^{-2}$), droplet density ($51.00 \text{ droplets cm}^{-2}$), and area coverage (15.77%) were highest in the upper layer as compared to middle layers ($0.75 \mu\text{L cm}^{-2}$, $19.33 \text{ droplets cm}^{-2}$, 10.25%, respectively) and bottom layers ($0.37 \mu\text{L cm}^{-2}$, $19.00 \text{ droplets cm}^{-2}$, 2.73%, respectively). The droplet penetrability was best in the upper layer, with the CV of deposition density reaching 6.34% when compared to the middle and bottom layers (6.45% and 13.02%, respectively).

Spray droplet is one of the most critical aspects affecting the droplet deposition rate, area coverage, and droplet density for insecticide spraying by UAV in the redgram field. There was higher droplet deposition rate ($1.79 \mu\text{L cm}^{-2}$), area coverage (16.17%)/ and droplet density ($48.00 \text{ droplets cm}^{-2}$) in the target area as compared to the non-target area (deposition rate: $0.39 \mu\text{L cm}^{-2}$, coverage: 3.54% and droplet density: $10.00 \text{ droplets cm}^{-2}$ respectively), which may have been due to the downwash air produced by the propeller

of the UAV sprayer. The downwash air velocity had effects on droplet deposition and the standing crop. Droplet deposition rate decreased as the lateral distance from the center of the UAV spray line increased (from $1.93 \pm 0.05 \mu\text{L cm}^{-2}$ to $0.22 \pm 0.05 \mu\text{L cm}^{-2}$), and similarly, the spray droplet drift distance was reduced with the increase in droplet size, which showed that the increase in spray droplet size can effectively minimize the spray droplet drift. The UAV spray method is quite effective, not only in terms of reach but also in mitigating health risks faced by farmers who walk through the fields with handheld sprayers, exposing themselves to toxic chemicals. Moreover, it will help to overcome the shortage of labor.

Author Contributions: Conceptualization, Y.D., K.R. and A.P.M.K.; methodology, Y.D., K.R., S.A. and S.B.; software, B.K.; validation, Y.D. and K.R.; formal analysis, Y.D., K.R. and S.B.; investigation, Y.D., K.R., S.A., S.B., A.P.M.K. and B.K.; resources, Y.D., S.B. and A.P.M.K.; data curation, Y.D., S.B. and A.P.M.K.; writing—original draft preparation, Y.D., K.R., S.B. and A.P.M.K.; writing—review and editing, K.R., S.A., S.B., B.K., A.P.M.K. and K.M.K.; visualization, Y.D., K.R., S.A. and S.B.; supervision, K.R., S.A. and K.M.K.; project administration, K.R., S.A. and K.M.K.; funding acquisition, K.R., S.A. and K.M.K. All authors have read and agreed to the published version of the manuscript.

Funding: This research was funded by Indian Council of Agricultural Research (ICAR), All India Coordinated Research Project (AICRP) on Farm Implements and Machinery (FIM), TNAU Coimbatore, Tamil Nadu.

Institutional Review Board Statement: Not applicable.

Informed Consent Statement: Not applicable.

Data Availability Statement: Not applicable.

Acknowledgments: The authors wish to acknowledge the financial assistance provided by the Indian Council of Agricultural Research (ICAR), All India Coordinated Research Project (AICRP) on Farm Implements and Machinery (FIM) and Tamil Nadu Agricultural University, Coimbatore, Tamil Nadu (India) for providing necessary research facilities for conducting the experiment.

Conflicts of Interest: The authors declare no conflict of interest.

References

- Wang, G.; Han, Y.; Li, X.; Andaloro, J.; Chen, P.; Hoffmann, W.C.; Han, X.; Chen, S.; Lan, Y. Field evaluation of spray drift and environmental impact using an agricultural unmanned aerial vehicle (UAV) sprayer. *Sci. Total Environ.* **2020**, *737*, 139793. [[CrossRef](#)]
- Huang, H.; Deng, J.; Lan, Y.; Yang, A.; Deng, X.; Zhang, L. A fully convolutional network for weed mapping of unmanned aerial vehicle (UAV) imagery. *PLoS ONE* **2018**, *13*, e0196302. [[CrossRef](#)]
- Yao, W.; Wang, X.; Lan, Y.; Jin, J. Effect of UAV prewetting application during the flowering period of cotton on pesticide droplet deposition. *Front. Agric. Sci. Eng.* **2018**, *5*, 455–461. [[CrossRef](#)]
- Xiongkui, H.; Bonds, J.; Herbst, A.; Langenakens, J. Recent development of unmanned aerial vehicle for plant protection in East Asia. *Int. J. Agric. Biol. Eng.* **2017**, *10*, 18–30.
- Kirk, I.W. Aerial spray drift from different formulations of glyphosate. *Trans. ASAE* **2000**, *43*, 555. [[CrossRef](#)]
- Ru, Y.; Zhou, H.; Jia, Z.; Wu, X.; Fan, Q. Design and application of electrostatic spraying system. *J. Nanjing For. Univ. (Nat. Sci. Ed.)* **2011**, *35*, 91–94.
- Huang, Y.; Hoffmann, W.C.; Lan, Y.; Wu, W.; Fritz, B.K. Development of a spray system for an unmanned aerial vehicle platform. *Trans. ASABE* **2009**, *25*, 803–809. [[CrossRef](#)]
- Bozdogan, N.Y. Assessment of buffer zone for aquatic organisms in pesticide application. *Int. J. Agric. Biol. Eng.* **2016**, *9*, 227–234.
- Yang, S.H.; Zheng, Y.J.; Liu, X.X. Research status and trends of downwash airflow of spray UAVs in agriculture. *Int. J. Precis. Agric. Aviat.* **2019**, *2*, 1–8. [[CrossRef](#)]
- Yang, S. Spray Droplet Deposition and Distribution Inside Crop Canopy and Control Efficiency Applied by Unmanned Aerial Vehicle. Ph.D. Thesis, Chinese Academy of Agricultural Sciences, Beijing, China, 2014; pp. 1–44. (In Chinese with English Abstract)
- Qing, T.; Ruirui, Z.; Liping, C.; Min, X.; Tongchuan, Y.; Bin, Z. Droplets movement and deposition of an eight-rotor agricultural UAV in downwash flow field. *Int. J. Agric. Biol. Eng.* **2017**, *10*, 47–56. [[CrossRef](#)]
- Wang, J.; Lan, Y.; Zhang, H.; Zhang, Y.; Wen, S.; Yao, W.; Deng, J. Drift and deposition of pesticide applied by UAV on pineapple plants under different meteorological conditions. *Int. J. Agric. Biol. Eng.* **2018**, *11*, 5–12. [[CrossRef](#)]
- He, X.; Zeng, A.; He, J. Effect of wind velocity from orchard sprayer on droplet deposit and distribution. *Nongye Gongcheng Xuebao (Trans. Chin. Soc. Agric. Eng.)* **2002**, *18*, 75–77.

14. Liu, X.J.; Zhou, H.P.; Zheng, J.Q. Research advances of the technologies for spray drift control of pesticide application. *Trans. CSAE* **2005**, *21*, 186–190.
15. Wang, X.; He, X.; Song, J.; Wang, Z.; Wang, C.; Wang, S.; Wu, R.; Meng, Y. Drift potential of UAV with adjuvants in aerial applications. *Int. J. Agric. Biol. Eng.* **2018**, *11*, 54–58. [[CrossRef](#)]
16. Smith, D.B.; Bode, L.E.; Gerard, P.D. Predicting ground boom spray drift. *Trans. ASAE* **2000**, *43*, 547. [[CrossRef](#)]
17. Fritz, B.K. Meteorological effects on deposition and drift of aerially applied sprays. *Trans. ASABE* **2006**, *49*, 1295–1301. [[CrossRef](#)]
18. Zhang, J.; He, X.; Song, J.; Zeng, A.; Liu, Y.; Li, X. Influence of spraying parameters of unmanned aircraft on droplets deposition. *Nongye Jixie Xuebao=Trans. Chin. Soc. Agric. Mach.* **2012**, *43*, 94–96.
19. An, J.; Xiang, W.; Han, Z.; Xiao, K.; Wang, Z.; Wang, X.; Li, Y. Validation of the Institute of Atmospheric Physics emergency response model with the meteorological towers measurements and SF6 diffusion and pool fire experiments. *Atmos. Environ.* **2013**, *81*, 60–67. [[CrossRef](#)]
20. Gao, Y.Y. Study on distribution of pesticide droplets in gramineous crop canopy and control effect sprayed by unmanned aerial vehicle. *Northeast Agric. Univ. Harbin, China* **2013**.
21. Li, J.; Lan, Y.; Shi, Y. Research progress on airflow characteristics and field pesticide application system of rotary-wing UAV. *Trans. Chin. Soc. Agric. Eng.* **2018**, *34*, 104–118.
22. Zhang, H.; Zheng, J.; Zhou, H.; Dorr, G.J. Droplet deposition distribution and off-target drift during pesticide spraying operation. *Nongye Jixie Xuebao=Trans. Chin. Soc. Agric. Mach.* **2017**, *48*, 114–122.
23. He, Y.; Wu, J.J.; Fang, H.; Zheng, Q.S.; Xiao, S.P.; Cen, H.Y. Research on deposition effect of droplets based on plant protection unmanned aerial vehicle: A review. *J. Zhejiang Univ. (Agric. Life Sci.)* **2018**, *44*, 392–398. (In Chinese)
24. Shengde, C.; Lan, Y.; Jiyu, L.; Zhiyan, Z.; Aimin, L.; Yuedong, M. Effect of wind field below unmanned helicopter on droplet deposition distribution of aerial spraying. *Int. J. Agric. Biol. Eng.* **2017**, *10*, 67–77.
25. Chen, S.; Lan, Y.; Zhou, Z.; Ouyang, F.; Wang, G.; Huang, X.; Cheng, S. Effect of droplet size parameters on droplet deposition and drift of aerial spraying by using plant protection UAV. *Agronomy* **2020**, *10*, 195. [[CrossRef](#)]
26. Hoffmann, W.C.; Hewitt, A.J. Comparison of three imaging systems for water-sensitive papers. *Appl. Eng. Agric.* **2005**, *21*, 961–964. [[CrossRef](#)]
27. Liu, Q.; Chen, S.; Wang, G.; Lan, Y. Drift Evaluation of a Quadrotor Unmanned Aerial Vehicle (UAV) Sprayer: Effect of Liquid Pressure and Wind Speed on Drift Potential Based on Wind Tunnel Test. *Appl. Sci.* **2021**, *11*, 7258. [[CrossRef](#)]
28. Berner, B.; Chojnacki, J. Use of drones in crop protection. In Proceedings of the IX International Scientific Symposium “Farm Machinery and Processes Management in Sustainable Agriculture”, Lublin, Poland, 22–24 November 2017.
29. Fritz, B.K.; Kirk, I.W.; Hoffmann, W.C.; Martin, D.E.; Hofman, V.L.; Hollingsworth, C.; McMullen, M.; Halley, S. Aerial application methods for increasing spray deposition on wheat heads. *Appl. Eng. Agric.* **2006**, *22*, 357–364. [[CrossRef](#)]
30. Lou, Z.; Xin, F.; Han, X.; Lan, Y.; Duan, T.; Fu, W. Effect of unmanned aerial vehicle flight height on droplet distribution, drift and control of cotton aphids and spider mites. *Agronomy* **2018**, *8*, 187. [[CrossRef](#)]
31. Dixon, D.; Boon, S.; Silins, U. Watershed-scale controls on snow accumulation in a small montane watershed, southwestern Alberta, Canada. *Hydrol. Process.* **2014**, *28*, 1294–1306. [[CrossRef](#)]
32. Salcedo, R.; Garcera, C.; Granell, R.; Molto, E.; Chueca, P. Description of the airflow produced by an air-assisted sprayer during pesticide applications to citrus. *Span. J. Agric. Res.* **2015**, *13*, e0208. [[CrossRef](#)]
33. Ling, W.; Du, C.; Mengchao, Z.; Yu, W.; Ze, Y.; Shumao, W. CFD simulation of low-altitude droplets deposition characteristics for UAV based on multi-feature fusion. *IFAC-Pap.* **2018**, *51*, 648–653. [[CrossRef](#)]
34. Li, J.; Shi, Y.; Lan, Y.; Guo, S. Vertical distribution and vortex structure of rotor wind field under the influence of rice canopy. *Comput. Electron. Agric.* **2019**, *159*, 140–146. [[CrossRef](#)]
35. Xinyu, X.; Kang, T.; Weicai, Q.; Yubin, L.; Huihui, Z. Drift and deposition of ultra-low altitude and low volume application in paddy field. *Int. J. Agric. Biol. Eng.* **2014**, *7*, 23–28.
36. Yang, F.; Xue, X.; Cai, C.; Sun, Z.; Zhou, Q. Numerical simulation and analysis on spray drift movement of multirotor plant protection unmanned aerial vehicle. *Energies* **2018**, *11*, 2399. [[CrossRef](#)]
37. Bergeron, V. Designing intelligent fluids for controlling spray applications. *Comptes Rendus Phys.* **2003**, *4*, 211–219. [[CrossRef](#)]
38. Choi, D.S.; Ma, K.C.; Kim, H.J.; Lee, J.H.; Oh, S.A.; Kim, S.G. Control standards of three major insect pests of Chinese cabbage (*Brassica campestris*) using drones for pesticide application. *Korean J. Appl. Entomol.* **2018**, *57*, 347–354.
39. Lan, Y.; Qian, S.; Chen, S.; Zhao, Y.; Deng, X.; Wang, G.; Qiu, X. Influence of the Downwash Wind Field of Plant Protection UAV on Droplet Deposition Distribution Characteristics at Different Flight Heights. *Agronomy* **2021**, *11*, 2399. [[CrossRef](#)]
40. Teske, M.E.; Bird, S.L.; Esterly, D.M.; Curbishley, T.B.; Ray, S.L.; Perry, S.G. AgDrift®: A model for estimating near-field spray drift from aerial applications. *Environ. Toxicol. Chem. Int. J.* **2002**, *21*, 659–671. [[CrossRef](#)]
41. Bilanin, A.J.; Teske, M.E.; Barry, J.W.; Ekblad, R.B. AGDISP: The aircraft spray dispersion model, code development and experimental validation. *Trans. ASAE* **1989**, *32*, 327–0334. [[CrossRef](#)]
42. Bache, D.H.; Sayer, W.J.D. Transport of aerial spray, I. A model of aerial dispersion. *Agric. Meteorol.* **1975**, *15*, 257–271. [[CrossRef](#)]
43. Miller, P.C.H.; Ellis, M.B. A review of spray generation, delivery to the target and how adjuvants influence the process. *Plant Prot. Q.* **1997**, *12*, 33–38.
44. Guo, S.; Li, J.; Yao, W.; Zhan, Y.; Li, Y.; Shi, Y. Distribution characteristics on droplet deposition of wind field vortex formed by multi-rotor UAV. *PLoS ONE* **2019**, *14*, 22–24. [[CrossRef](#)]

45. Martin, D.; Singh, V.; Latheef, M.A.; Bagavathiannan, M. Spray deposition on weeds (Palmer amaranth and Morningglory) from a remotely piloted aerial application system and backpack sprayer. *Drones* **2020**, *4*, 59. [[CrossRef](#)]
46. Wen, S.; Zhang, Q.; Yin, X.; Lan, Y.; Zhang, J.; Ge, Y. Design of plant protection UAV variable spray system based on neural networks. *Sensors* **2019**, *19*, 1112. [[CrossRef](#)]
47. S386; ASABE Standards. Spray Nozzle Classification by Droplet Spectra—Forages. ASABE: St. Joseph, MI, USA, 2004.
48. Zhu, H.; Salyani, M.; Fox, R.D. A portable scanning system for evaluation of spray deposit distribution. *Comput. Electron. Agric.* **2011**, *76*, 38–43. [[CrossRef](#)]
49. Whitney, R.W.; Gardisser, D.R. *DropletScan Operators Manual*; WRK of Oklahoma and WRK of Arkansas: Stillwater, OK, USA, 2003.
50. Martin, D.E. A fluorescent imaging technique for quantifying spray deposits on plant leaves. *At. Sprays* **2014**, *24*, 367–373. [[CrossRef](#)]
51. Zhang, X.Q.; Song, X.P.; Liang, Y.J.; Qin, Z.Q.; Zhang, B.Q.; Wei, J.J.; Li, Y.R.; Wu, J.M. Effects of spray parameters of drone on the droplet deposition in sugarcane canopy. *Sugar Tech* **2020**, *22*, 583–588. [[CrossRef](#)]
52. S386.2; ASABE Standards. Calibration and Distribution Pattern Testing of Agricultural Aerial Application Equipment. ASABE: St. Joseph, MI, USA, 2018.
53. Yang, Z.; Qi, L.; Wu, Y. Influence of UAV rotor down-wash airflow for droplet penetration. In *2018 ASABE Annual International Meeting*; American Society of Agricultural and Biological Engineers: St. Joseph, MI, USA, 2018; p. 1.
54. Fengbo, Y.; Xinyu, X.; Ling, Z.; Zhu, S. Numerical simulation and experimental verification on downwash air flow of six-rotor agricultural unmanned aerial vehicle in hover. *Int. J. Agric. Biol. Eng.* **2017**, *10*, 41–53. [[CrossRef](#)]
55. Wen, S.; Han, J.; Ning, Z.; Lan, Y.; Yin, X.; Zhang, J.; Ge, Y. Numerical analysis and validation of spray distributions disturbed by quad-rotor drone wake at different flight speeds. *Comput. Electron. Agric.* **2019**, *166*, 105036. [[CrossRef](#)]
56. Zheng, Y.; Yang, S.; Liu, X.; Wang, J.; Norton, T.; Chen, J.; Tan, Y. The computational fluid dynamic modeling of downwash flow field for a six-rotor UAV. *Front. Agric. Sci. Eng.* **2018**, *5*, 159–167. [[CrossRef](#)]
57. Yang, S.; Liu, X.; Chen, B.; Li, S.; Zheng, Y. CFD models and verification of the downwash airflow of an eight-rotor UAV. In *2019 ASABE Annual International Meeting*; American Society of Agricultural and Biological Engineers: St. Joseph, MI, USA, 2019; p. 1.
58. Bird, S.L.; Esterly, D.M.; Perry, S.G. *Off-Target Deposition of Pesticides from Agricultural Aerial Spray Applications*; American Society of Agronomy, Crop Science Society of America, Soil Science Society of America: Madison, WI, USA, 1996; Volume 25, pp. 1095–1104.
59. Nuyttens, D.; De Schampheleire, M.; Baetens, K.; Sonck, B. The influence of operator-controlled variables on spray drift from field crop sprayers. *Trans. ASABE* **2007**, *50*, 1129–1140. [[CrossRef](#)]
60. Ferguson, J.C.; Chechetto, R.G.; Hewitt, A.J.; Chauhan, B.S.; Adkins, S.W.; Kruger, G.R.; O'Donnell, C.C. Assessing the deposition and canopy penetration of nozzles with different spray qualities in an oat (*Avena sativa* L.) canopy. *Crop Prot.* **2016**, *81*, 14–19. [[CrossRef](#)]
61. Hoffmann, W.C.; Hewitt, A.J.; Barber JA, S.; Kirk, I.W.; Brown, J.R. *Field Swath and Drift Analyses Techniques*; Paper Number: AA03-007; U.S. Department of Agriculture: Washington, DC, USA, 2003.